Supporting Information

Phase Behavior of Poly(2-vinyl pyridine)-*block*-Poly(4-vinyl pyridine) Copolymers Containing Gold Nanoparticles

Jaeyong Lee, Jongheon Kwak, Chungryong Choi, Sung Hyun Han, and Jin Kon Kim*

National Creative Research Initiative Center for Smart Block Copolymers, Department of Chemical Engineering, Pohang University of Science and Technology, Pohang, Kyungbuk 790-784, Republic of Korea.

*Corresponding author. E-mail: jkkim@postech.ac.kr; Fax: (+) 82-54-279-8298

S1. The reduction from gold precursor to gold nanoparticle

We prepared poly(2-vinyl pyridine)-*block*-poly(4-vinyl pyridine) (P24VP) containing gold nanoparticles as follows. A predetermined amount of gold precursor ($HAuCl_4$) was added to P24VP in THF, and thermally annealed at 210 ºC for 12 h. The complete reduction from gold precursor to gold nanoparticle after thermal annealing was confirmed through X-ray photoelectron spectroscopy (XPS) measurement. Fig. S1 (a)–(b) gives XPS profiles of P24VP with gold nanoparticles before and after thermal annealing. Two peaks corresponding to Au^{3+} were located at 85.4 and 89.0 eV (Fig. S1 (a)). After thermal annealing, these peaks were shifted to 84.5 and 88.1 eV assigned to Au $4f_{7/2}$ and Au $4f_{5/2}$, respectively (Fig. S1 (b)).[1.] Crystal structure of gold nanoparticles was characterized by X-ray diffraction (MXP18-HF, MAC SCIENCE CO) (Fig. S1 (c)). Intense diffraction peaks are observed at 38.2º, 44.4º, which correspond to (1 1 1) and (2 0 0) reflections of gold crystals, respectively.

In addition, we measured the amount of chloride in the sample by using combustion ion chromatography (CIC; Dionex ICS-5000, Mitsubishi AQF-2100Ht) for P24VP-L[0.04]. Figure S1 (d) showed chromatogram of P24VP-L[0.04] before and after thermolysis at 210 ºC for 12 h. The measured amount of chloride in P24VP-L[0.04] before thermolysis was 2.8 wt %, close to the initially coordinated amount (2.7 wt%). After thermolysis, the remaining chloride in the sample was only 0.15 wt%, which means that more than 95 % of chloride in the sample disappeared. This is fully consistent with a previous result.[2] Namely, during thermolysis of P24VP coordinated with $HAuCl_4$, the chloride in the sample was removed as gas state of HCl and Cl_2 based on the following reaction.

$$\mathrm{P24VP} - H^+ + [AuCl_4]^- \xrightarrow{\Delta} Au^0 + HCl(g) + Cl_2(g)$$

It is noted that HCl and Cl_2 gases were easily removed because of using a vacuum oven during thermolysis.

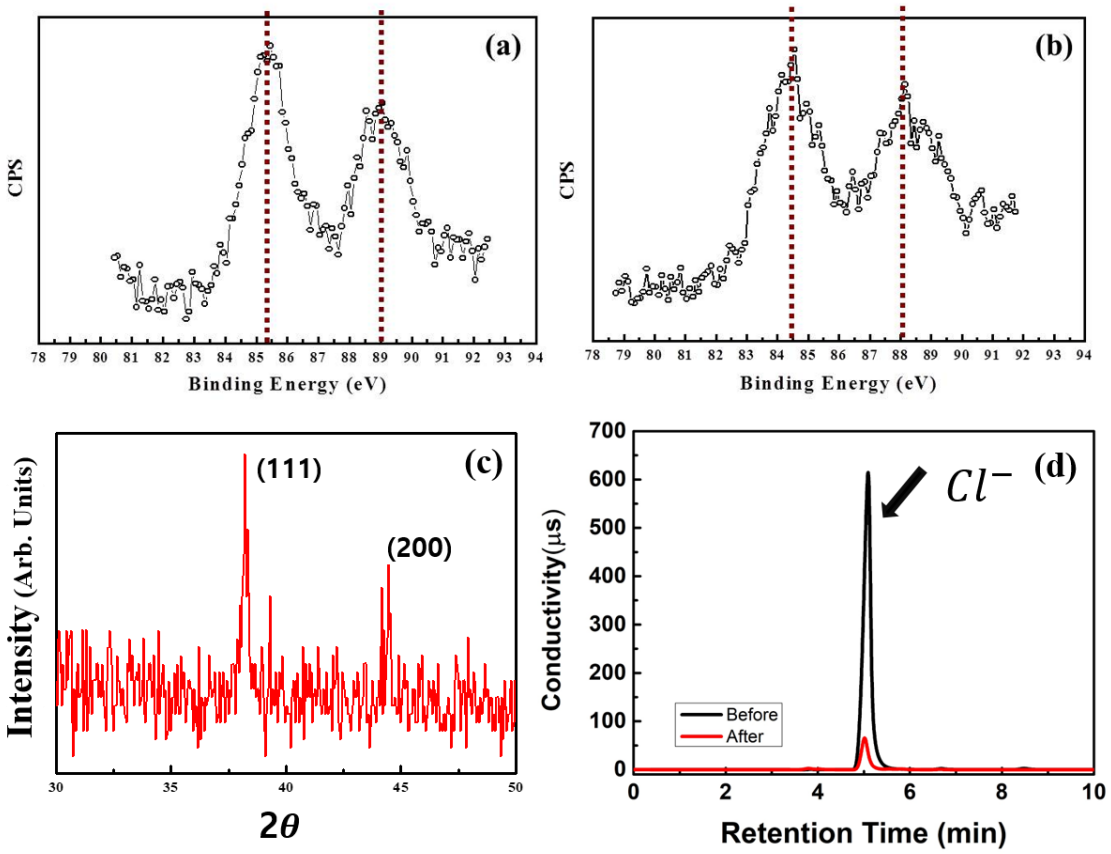

Fig. S1. XPS profiles of P24VP with gold nanoparticles (a) before and (b) after thermal annealing. (c) XRD profile of prepared gold nanoparticles. (d) CIC chromatography of P24VP-L[0.04] before and after thermolysis 210 ^{o}C for 12 h.

S2. Rheological measurement during two heating runs.

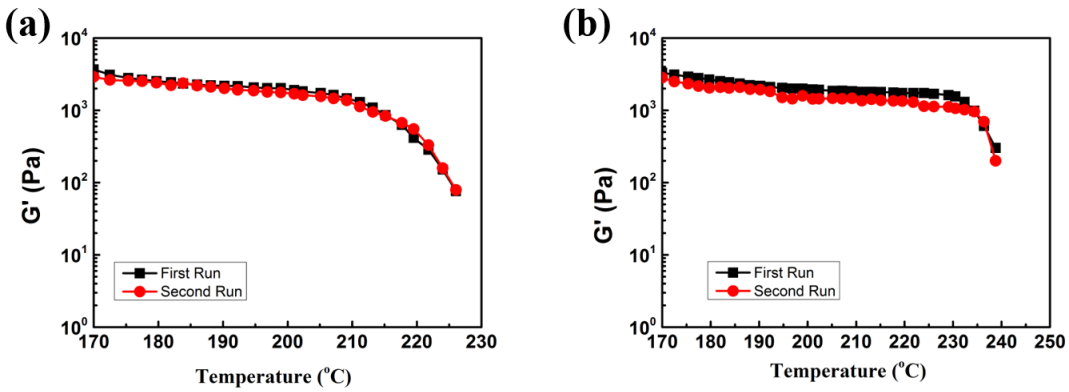

Fig. S2. Temperature dependence of G′ of P24VP-L[0.02] (a) and P24VP-L[0.03] (b) obtained during two heating runs.

To confirm that the measured T_{ODT} represents equilibrium phenomenon, we carried out rheological measurement using two heating runs for two samples (P24VP-L[0.02] and P24VP-L[0.03]) which showed unusual change in T_{ODT}. We carried out the second heating run after performing the first heating run followed by thermal annealing again at 200 °C for 12 h. As shown in Fig. S2, the T_{ODT}s of both samples obtained during the second heating run are essentially the same as those obtained during the first heating run. Thus, the measured T_{ODT}s correspond to thermal equilibrium, not kinetic trapping**.**

S3. Small-angle X-ray scattering (SAXS) profiles of P24VP with various amounts of gold nanoparticles

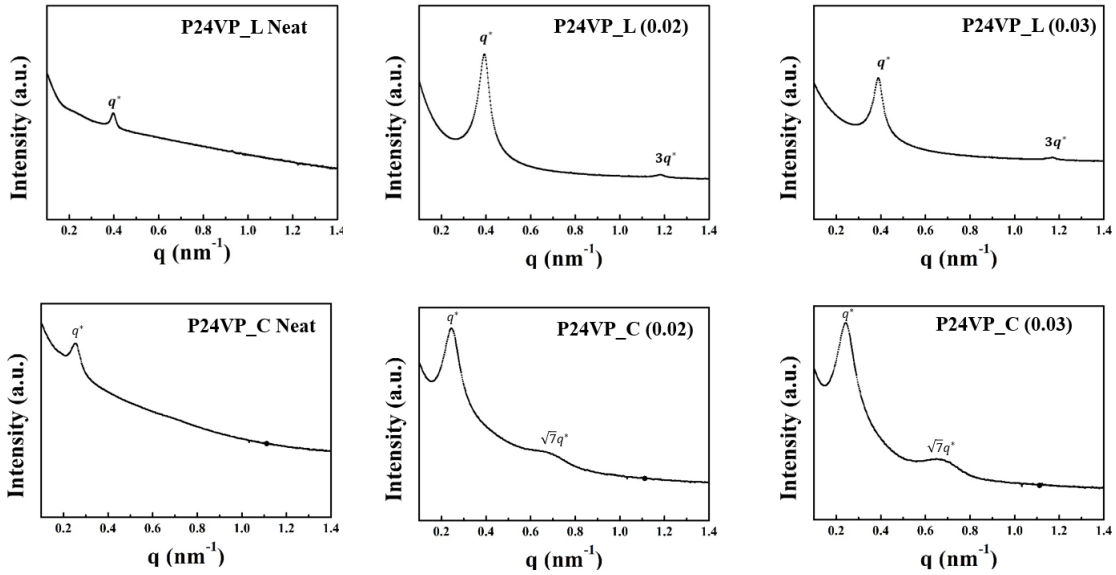

Fig. S3. SAXS profiles at 210 ºC of P24VP-L and P24VP-C without and with two different molar ratios (0.02 and 0.03) of gold precursor to 4VP monomer (r_{gold} = [$HAuCl_4$]/[4VP]).

Fig. S3 SAXS profiles of P24VP-L and P24VP-C without and with two different molar ratios (0.02 and 0.03) of gold precursor to 4VP monomer (r_{gold} = [$HAuCl_4$]/[4VP]). Neat P24VP-L and P24VP-C exhibited only a single first SAXS peak. This is because of small electron density difference between 2-vinylpyridine (2VP) and 4-vinylpyridine (4VP). But with the addition of gold nanoparticles in P24VP, higher order SAXS peaks were observed at 3q* for P24VP-L and √7q* for P24VP-C containing gold nanoparticles, respectively. This implies that the gold nanoparticles are not equally distributed in both P2VP and P4VP microdomains. If the gold nanoparticles had been equally located in both microdomains, high order SAXS peak would not be observed, like neat P24VP.

S4. T_{ODT} measurements for Polystyrene-*block*-poly(4-vinyl pyridine) (PS4VP) and Polystyrene-*block*-poly(2-vinyl pyridine) (PS2VP) with various amounts of gold nanoparticles.

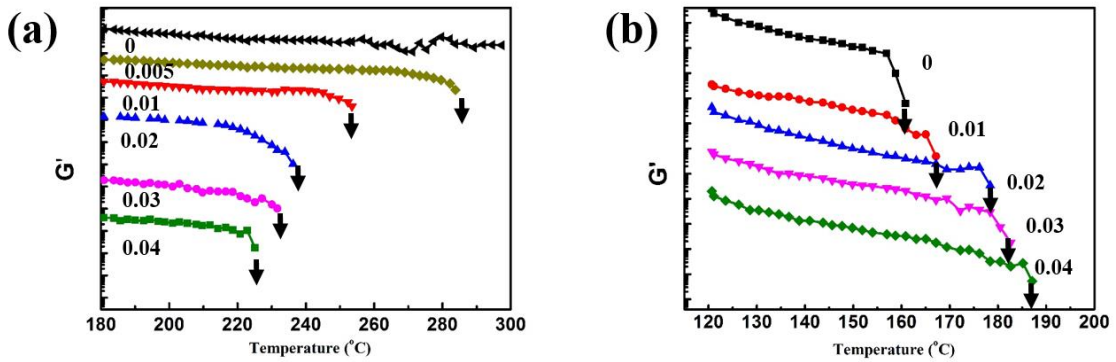

Fig. S4. Temperature dependence of G' at ω = 0.1 rad/s for (a) PS4VP and (b) PS2VP with various values of r_{gold}. Here, r_{gold} = $[HAuCl_4]/[4VP]$ for PS4VP, while it is $[HAuCl_4]/[2VP]$ for PS2VP.

Fig. S4 gives temperature dependence of G' for PS4VP and PS2VP with various values of r_{gold}. With increasing the amount of gold nanoparticle (r_{gold}) up to 0.04, the T_{ODT} of PS4VP containing gold nanoparticles gradually decreased, while that of PS2VP containing gold nanoparticles gradually increased.

S5. Tg measurements

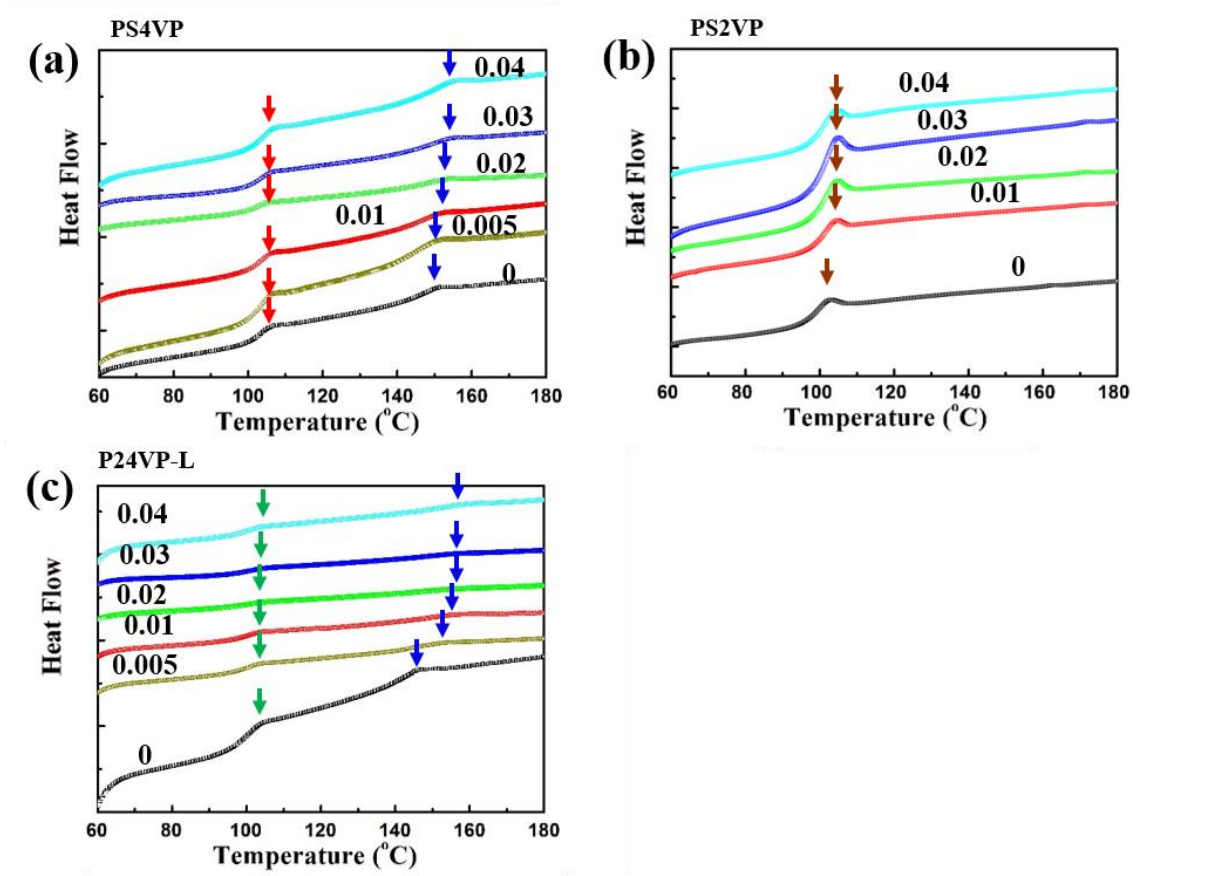

Fig. S5. DSC thermograms for three different block copolymers: (a) PS4VP, (b) PS2VP, and (c) P24VP-L with various values of r_{gold}. Here, r_{gold} = $[HAuCl_4]$/[4VP] for PS4VP and P24VP-L, while it is $[HAuCl_4]$/[2VP] for PS2VP.

Fig. S5 gives DSC thermograms for three different block copolymers containing various values of $\mathbf{r}_{gold}$. PS4VP and P24VP with various amounts of gold nanoparticles clearly showed two distinct T_gs corresponding to each block (Fig.S5 (a) and S5 (c)). Red, blue, and green arrows represent T_g of PS, P4VP, and P2VP block, respectively. The appearance of two T_gs implies that all the samples are microphase-separated. However, for PS2VP containing gold nanoparticles, it is almost impossible to distinguish T_g between PS and P2VP blocks due to similar values of T_g (brown arrow in Figure S5), though those samples become microphase-separated.

S6. Change of the lamellar domain spacing with the amount of gold nanoparticles

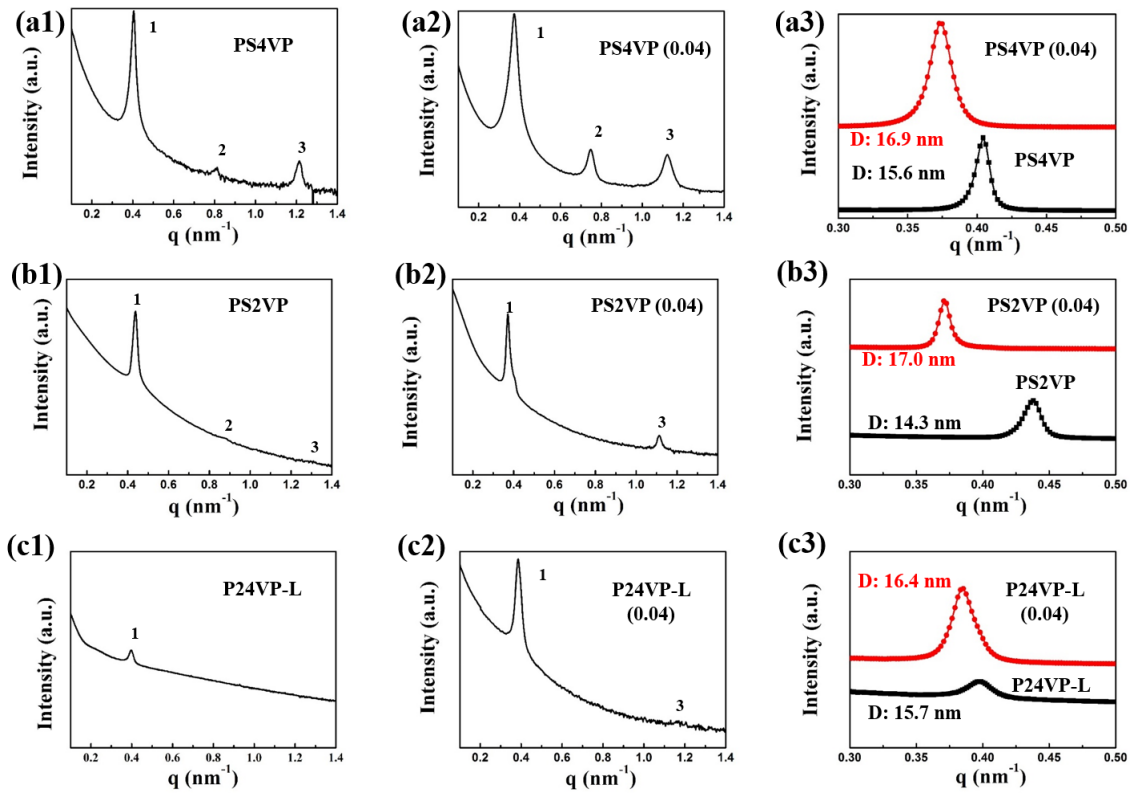

Fig. S6. SAXS profiles of PS4VP ((a1)-(a2)), PS2VP ((b1)-(b2)) and P24VP-L((c1)-(c2)) without and with r_{gold} = 0.04. The right panels represent the change of the first order peak of each block copolymer.

Fig. S6 gives SAXS profiles of PS4VP, PS2VP, and P24VP-L without and with r_{gold} = 0.04. The lamellar domain spacing ($D = 2\pi/q^*$, in which q^* is the first peak position) of all block copolymers with gold nanoparticles was larger than that of neat block copolymers. Among three different block copolymers, PS2VP showed the largest increase in D after gold nanoparticles were incorporated, which indicates that the chain stretching of P2VP chains is much larger than that of P4VP chains. This is because of larger steric hindrance during the coordination of the ortho position of nitrogen in the pyridine ring of P2VP chains with gold precursors compared with that of the para position of nitrogen of P4VP chains.

S7. High-Angle annular dark-field scanning transmission electron microscopy (HAADF-STEM) and bright-field scanning transmission electron microscopy (BF-STEM).

Fig. S7 gives HAADF-STEM and BF-STEM images for P24VP-L with two different values of r_{gold} (0.02 and 0.04). When the staining time of I_2 vapor is 40 min, a distinct contrast is observed between P2VP and P4VP microdomains because of selective I_2 staining of P4VP microdomain. Thus, P4VP microdomains look white in dark-field STEM image,[3,4] while they look dark in bright-field STEM image. Although P4VP microdomains look white in dark field image, gold nanoparticles marked by blue circle show much brighter white color than P4VP microdomains. Of course, in a bright field image, gold nanoparticles look the darkest. From Fig. S7 (a1) and (a2), the brightest spots were observed in P4VP microdomain in HAADF-STEM image, while those correspond to the darkest spots in BF-STEM image. Thus, this clearly indicates that gold nanoparticles were located only in P4VP microdomains for P24VP-L[0.02]. For P24VP-L[0.04], gold nanoparticles were observed at both microdomains: P2VP (green circle) and P4VP (blue circle) microdomains. Nevertheless, the amount of gold nanoparticles in P4VP microdomain is much larger than that in P2VP microdomains, which causes to re-decrease the $T_{ODT.}$

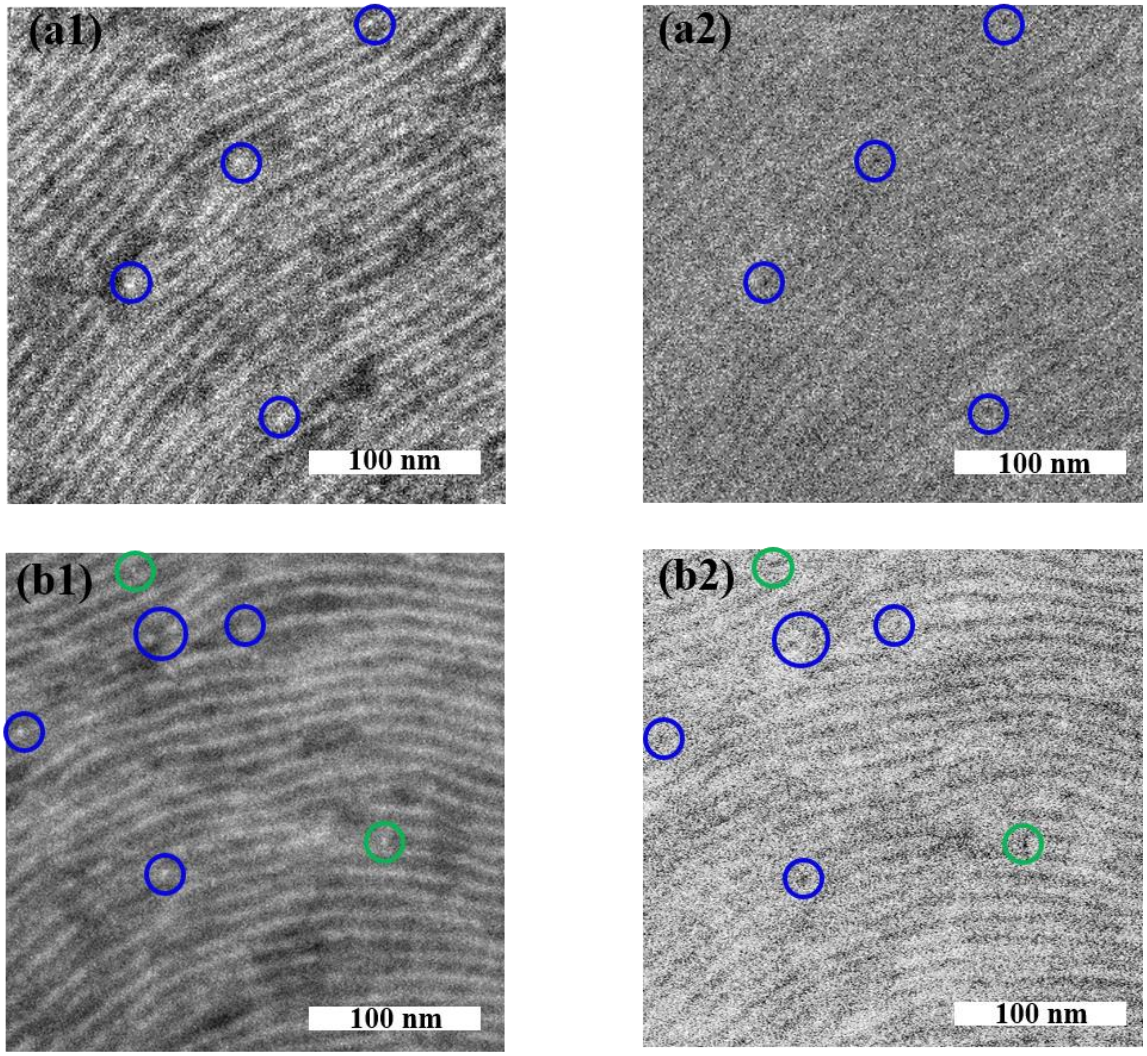

Fig. S7. HAADF-STEM (left panels) and BF-STEM (right panels) images for P24VP-L[0.02] ((a1) and (a2)) and P24VP-L[0.04] ((b1) and (b2)). Blue and green circles indicate gold nanoparticles located inside P4VP and P2VP microdomains, respectively.

References

(1) Zuruzi, A. S.; Ward, M. S.; MacDonald, N. C. Fabrication and characterization of patterned micrometre scale interpenetrating Au-TiO_2 network nanocomposites. *Nanotechnology* **2005**, *16*, 1029-1034.

(2) Mendoza, C.; Pietsch, T.; Gutmann, J. S.; Jenichen, D.; Gindy, N.; Fahmi, A. Block Copolymers with Gold Nanoparticles: Correlation between Structural Characteristics and Mechanical Properties. *Macromolecules* **2009**, *42*, 1203-1211.

(3) Shin, D. O.; Mun, J. H.; Hwang, G. T.; Yoon, J. M.; Kim, J. Y.; Yun, J. M.; Yang, Y. B.; Oh, Y.; Lee, J. Y.; Shin, J.; Lee, K. J.; Park, S.; Kim, J. U.; Kim, S. O. Multicomponent Nanopatterns by Directed Block Copolymer Self-Assembly. *ACS Nano* **2013**, *7*, 8899-8907.

(4) Wang, Y.; Turak, A.; Manners, I.; Winnik, M. A. Interfacial Staining of a Phase –Separated Block Copolymer with Ruthenium Tetroxide. *Macromolecules* **2007**, *40*, 1594-1597.